Macromolecules

Volume 23, Number 19 September 17, 1990

Theory of Micelle Formation by Amphiphilic Side-Chain Polymers

Esam Hamad and Syed Qutubuddin*

Departments of Chemical Engineering and Macromolecular Science, Case Western Reserve University, Cleveland, Ohio 44106

Received July 11, 1989

ABSTRACT: A microscopic model for the formation of micelles by amphiphilic side-chain polymers is developed. The model predicts the free energy, the size of the micelles, and the micellar phase composition. Characteristic values are calculated for the number of backbone segments and the length of the hydrophobic side chains beyond which only single molecule micelles form. The effects of salt concentration, polymer volume fraction, and polymer dimensions on the composition of the micellar phase and micelle size distribution are discussed.

1. Introduction

The motivation for this work is the growing interest in polymer surfactant interactions.[1-5] Such interactions are of special importance when the polymer is amphiphilic in nature. Before one can model the combined system of surfactant and polymer in aqueous solution, a good understanding of the behavior of amphiphilic polymers in water is needed. The effects of various molecular forces and solution properties on the formation of polymer micelles are discussed in this article.

A number of experimental studies on amphiphilic polymers in water have been published.[6-17] The early work on polysoaps covered both ionic[6,7] and nonionic[8] polymers and has been reviewed by Bekturov and Bakauova.[9] Finkelmann et al.[10] synthesized a number of liquid-crystalline surfactants and then attached them as side chains to a siloxane backbone. Both monomeric and polymeric surfactants were found to form rodlike micelles. However, phase behavior investigation showed that the polymeric micelles are more stable, possibly due to the restricted movement of the surfactant side chains. The formation of normal or inverted spherical, rodlike and disklike micelles was also discussed in light of the different location of the hydrophobic group relative to the backbone.[11]

To study the effects of hydrophobic side-chain length, the separation distance between side chains, and electrostatic forces on micelle formation, three series of ionenes were synthesized, and the viscosities of their solutions in water and water–ethanol mixtures were measured.[12,13] The backbones in these polymers carry well-defined charges and incorporate alkyl side chains of varying lengths. For small side chains, the polymer behaves as a polyelectrolyte, but, as the length of the side chain increases, the polymer starts to form micelles. More compact micelles are formed in solvents with higher polarity. The onset of micelle formation was found to be less affected by charge density than the length of the alkyl side chains.[12,13]

Other studies of amphiphilic polymers in aqueous solutions include the work of Schulz et al.[15] and Valint and Bock.[16] These studies showed that at low polymer concentrations a compact structure is formed by a single chain, while at higher concentrations intermolecular interactions cause the formation of large species. The formation of spherical and wormlike polymer micelles was also investigated in organic solvents.[17]

Compared to experimental work, little has been done in modeling amphiphilic branched polymers. In an early work on polysoaps, Nakagawa and Inoue[18] assumed that association occurs only between neighboring groups and discussed the conditions for formation of intermolecular and intramolecular micelles. Intramolecular association has been studied in model chains[19,20] and in DNA molecules.[21] Aggregation of idealized two-dimensional chains has been studied using computer simulation.[22] The second virial coefficient for a dilute solution of polymers containing saturating two-body groups, i.e., "stickers", has been calculated.[23]

Leibler et al.[24] modeled the formation of spherical micelles in mixtures of block copolymers and homopolymers. This model was extended to include triblock copolymers.[25] Munch and Gast[26] used the same model to study micelle formation by block copolymers with small insoluble headgroups in a solution of small solvent molecules. Their study covered both spherical and lamellar micelles, and the predicted regimes of each type were identified. Halperin[27] exploited the similarity between star

* To whom correspondence should be addressed.

0024-9297/90/2223-4185$02.50/0

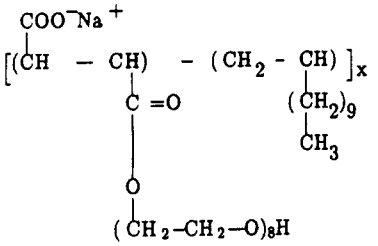

Figure 1. Structure of the model polymer.

polymers and polymeric micelles to derive scaling laws for the micelle size.

The polymers considered in this work have a comblike structure with both hydrophilic and hydrophobic side chains. An example of such polymers is Dapral GE 202 Na (Akzo Chemie), which is a maleic anhydride α-olefin copolymer. A model polymer used for thermodynamic calculations is shown in Figure 1. The backbone of this polymer consists of carbon atoms, with both hydrophobic and hydrophilic pendant groups distributed uniformly along the backbone. The amphiphilic nature of polymers such as this induces the formation of micelles. The free energy of a single micelle of polymer with comblike structure is calculated in section 2, the micellar phase properties are calculated in section 3, and the effects of salt concentration, hydrocarbon chain length, number of polymer segments and polymer concentration on the micellar phase are discussed in section 4.

2. Formation of Micelles

The amphiphilic branched polymer molecules are assumed to form spherical micelles. Although other shapes, such as rods or disks, and liquid-crystalline phases are possible under the appropriate conditions, spherical micelles are formed by some polymers such as Dapral GE 202 Na. Preliminary light-scattering and TEM studies on this polymer indicate that spherical micelles form at low concentrations.[28] Also the viscosity of the aqueous solution is low. Even at 10% (w/w) polymer, the apparent viscosity is only about 2 cP, clearly indicating that there is no entanglement.[28] Entanglement would be expected at the higher polymer concentrations if the micelles were elongated or rodlike. The thermodynamics of nonspherical micelles will be published separately.[29]

In the present model, the core of the spherical micelle is formed by the hydrophobic side chains. The number of these side chains is assumed large enough, and their separation distance is assumed small enough, such that single molecules always form monomolecular micelles. For example, the number of side chains for the model polymer depicted in Figure 1 is varied between 15 and 45 while the separation between the side chains is kept at four C–C bonds. The polymer backbone is distributed in a spherical shell around the core as shown in Figure 2. The radius of the hydrocarbon core is b, and the thickness of the shell occupied by the backbone is D. The hydrophilic side chains, which are connected to the polymer backbone, extend toward the bulk solution. Since the backbone configurational entropy is affected by the shell thickness, D is allowed to vary in the optimization of the overall free energy. For simplicity it is assumed that the backbone is restricted to the shell and uniformly distributed over that region. The assumption that the backbone does not penetrate the core is expected to hold for moderate size polymer molecules with strongly hydrophilic side chains such as ethylene oxide.

The driving force for the formation of micelles is the reduction in free energy when the hydrophobic side chains lose contact with water. On the other hand, a number of forces oppose the micelle formation. The balance between these forces determines the types and properties of the micelles formed. Therefore, the first step in studying micelle formation should be modeling the free energy. The free energy of a micelle of m polymer molecules is denoted by F_m. The difference between F_m and the reference state free energy, $F_{m,o}$, is written as the sum of four contributions

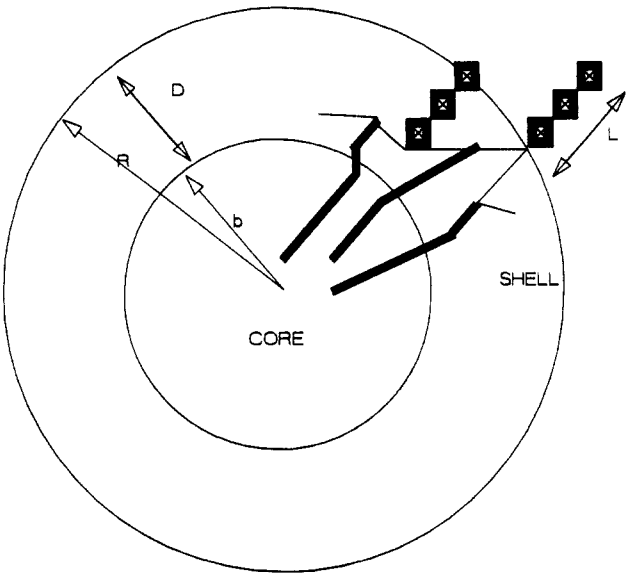

Figure 2. Geometry of a single micelle. The squares represent the hydrophilic groups, and the thick lines represent the hydrophobic side chains. The core contains hydrophobic side chains only. The spherical shell contains the polymer backbone, part of the side chains, and solvent.

$$F_m - F_{m,o} = F_{core} + F_{surf} + F_{conf} + F_{int} \quad (1)$$

where F_{core} is the free energy of formation of the hydrocarbon core, F_{surf} is the interfacial energy, F_{conf} is the free energy of confining the backbone in a spherical shell of thickness D, and F_{int} is the free energy due to interactions among backbone segments. $F_{m,o}$ accounts for contributions that do not change with micelle size and do not alter the driving force for intermolecular association. The driving force is the difference $(mF_1 - F_m)$, where F_1 is the free energy of a monomolecular micelle. The free energy loss due to orientational restriction of the hydrophilic side chains is one example of these contributions. The four contributions on the right-hand side of eq 1 are individually modeled next.

2.1. Hydrocarbon Core. Consider a backbone segment at a distance r from the center ($r \geq b$). A hydrophobic side chain is attached to this segment. The length of the side chain in the core is $l + b - r$ where l is the length of the hydrophobic side chain. The number of segments at r is $\eta 4\pi r^2\, dr$ where η is the segment density:

$$\eta = Nm/(4\pi/3)(R^3 - b^3) \quad (2)$$

In this equation N is the number of segments per molecule, m is the number of molecules in a micelle, and $R = b + D$. Let μ be the energy of transferring a side chain from an aqueous environment to the hydrocarbon core. The free energy F_{core} is then

$$F_{core} = \int_b^{b+D} \frac{\mu}{l}(l + b - r)\eta 4\pi r^2\, dr \qquad D \leq l \quad (3a)$$

$$F_{core} = \int_b^{b+l} \frac{\mu}{l}(l + b - r)\eta 4\pi r^2\, dr \qquad D \geq l \quad (3b)$$

The core radius, b, and the shell thickness, D, can be related by assuming that the core is incompressible. If the

volume of a hydrophobic side chain is v_s, then the volume of the core, $(4\pi/3)b^3$, is equal to

$$(4\pi/3)b^3 = \int_b^{b+D} \frac{v_s}{l}(l + b - r)\eta 4\pi r^2\, dr \qquad D \le l \tag{4a}$$

$$(4\pi/3)b^3 = \int_b^{b+l} \frac{v_s}{l}(l + b - r)\eta 4\pi r^2\, dr \qquad D \ge l \tag{4b}$$

Combining eq 3 and eq 4 gives

$$F_{core} = \frac{4\pi}{3}\frac{b^3}{v_s}\mu \tag{5}$$

Carrying out the integrations in eq 4 and extracting the root at $D = 0$ give

$$3R^3 + (V_r b^3/l^2 - 4l - b)[R^2 + bR + b^2] = 0 \qquad D \le l \tag{6a}$$

$$R = l\left\{\frac{(1 + b/l)^4}{V_r(b/l)^3} - \frac{4 + b/l}{V_r} + (b/l)^3\right\}^{1/3} \qquad D \ge l \tag{6b}$$

where $V_r = 16\pi l^3/(3mNv_s)$.

2.2. Interfacial Energy. The residual contact between water molecules in the shell region and the surface of the hydrophobic core results in a positive contribution to the free energy. The area of contact is the total surface of the core ($4\pi b^2$) less the sum of the cross-sectional areas of the hydrophobic side chains. The interfacial energy can be calculated if the interfacial tension, γ, is known

$$F_{surf} = \gamma(4\pi b^2 - A_H) \tag{7}$$

where A_H is the cross-sectional area of the hydrocarbon side chain ($A_H < 4\pi b^2$) given by

$$A_H = mN\frac{v_s}{l} \qquad D \le l \tag{8a}$$

$$A_H = mN\frac{v_s}{l}\frac{l^3 - b^3}{R^3 - b^3} \qquad D \ge l \tag{8b}$$

The interfacial tension is assumed to be the same as for a planar interface between a bulk polymer solution and a hydrocarbon.

2.3. Confinement of the Backbone. In the current model the backbone is confined to a spherical shell of thickness D. The loss of configurational entropy due to this confinement can be calculated using the self-consistent-fields approach. For an ideal chain, the eigenvalue problem of this approach reduces to[30]

$$-\frac{a^2}{6}\nabla^2 u_i = \omega_i u_i \tag{9a}$$

$$u_i(b) = u_i(R) = 0 \tag{9b}$$

where a is the backbone segment length, u_i is the ith eigenfunction in the partition function expansion,[30] and ω_i is the corresponding eigenvalue. This eigenvalue problem occurs frequently in physical systems. It has been solved, for example, in the context of heat conduction in a spherical shell.[31] The eigenvalues are $\omega_i = (1/6)(i\pi a/D)^2$. Assuming ground-state dominance, the entropy of confining one molecule is

$$\Delta S/k = -(\pi^2/6)N(a/D)^2 \tag{10}$$

Confinement of m molecules in the shell results in the following energy change:

$$F_{conf} = -T\Delta S = kTmN(\pi^2/6)(a/D)^2 \tag{11}$$

The validity of assuming ground-state dominance can be verified by calculating the error in ignoring higher order terms in the partition function. This error is of the order $\exp\{-N(\omega_2 - \omega_1)\}$.[30] For $D \approx l$ and $N = 15$ the error is approximately 10^{-5} in units of kT, very small compared to the free energy values reported in Table II.

2.4. Interaction Free Energy. The interactions between polymer segments in the shell result from van der Waals forces and also electrostatic forces if the backbone carries ionic groups. The van der Waals forces can be accounted for by using a virial expansion

$$\frac{F_{vw}}{kT} = \int\left[\frac{v}{2}\eta^2 + \frac{w}{6}\eta^3\right]4\pi r^2\, dr = \left[\frac{v}{2}\eta^2 + \frac{w}{6}\eta^3\right]\frac{4\pi}{3}(R^3 - b^3) \tag{12}$$

where v is related to the volume of the polymer skeleton (per segment) in the shell, v_o, and the Flory interaction parameter, χ, by

$$v = v_o(1 - 2\chi) \tag{13}$$

For polymers in good solvents away from the Θ temperature the third virial term can be neglected, and eq 12 reduces to

$$\frac{F_{vw}}{kT} = \frac{3v_o}{8\pi}(1 - 2\chi)\frac{m^2N^2}{R^3 - b^3} \tag{14}$$

The volume v_o consists of the backbone segment and part of the hydrophobic and hydrophilic side chains.

The volume of the part of hydrophobic chain in the shell is $v_s - 4\pi b^3/3mN$. The volume of the backbone segment is v_B. The volume of the part of hydrophilic side chain in the shell is $(v_p/mNL)\eta\int(R - r)\, 4\pi r^2\, dr$, where v_p is the volume of a hydrophilic side chain and L its length. The volume v_o is finally given by

$$v_o = v_s - \frac{4\pi b^3}{3mN} + v_B + \frac{v_p}{4L}\frac{1}{R^3 - b^3}[R^4 - b^3(4D + b)] \qquad D \le L \tag{15}$$

The electrostatic free energy can be calculated from the Poisson–Boltzmann equation with appropriate approximations. Assuming that the charge is uniformly distributed over the shell, the Poisson–Boltzmann equation takes the form

$$\nabla^2\Psi = -\frac{e}{\epsilon}(\beta\eta + C_s\exp(-e\Psi/kT) - C_s\exp(e\Psi/kT)) \tag{16}$$

where Ψ is the electrostatic potential, e is the electron charge, ϵ is the dielectric constant of the solvent, C_s is the salt concentration, and β is the fraction of backbone segments carrying a charge. This equation was solved using the Debye–Hückel approximation for the same geometry considered here.[32] However, it was shown analytically[33] and by comparison to exact numerical solution[34] that the Donnan approximation is much better in this case.

The Donnan approximation is equivalent to setting $\nabla^2\Psi$ equal to zero. The potential, under this approximation, is[33]

$$\frac{e\Psi_o}{kT} = \sinh^{-1} f \tag{17}$$

where $f = C/2C_s$ and $C = \beta\eta$ is the concentration of fixed

charges. The free energy is then[35]

$$\frac{F_{el,o}}{kT} = \int 4\pi r^2 \, dr \int_0^C \frac{e\Psi_o}{kT} \, dC = \beta m N \left[\sinh^{-1} f - \frac{(1+f^2)^{1/2} - 1}{f} \right] \quad (18)$$

A correction to eq 17, which can bring the electrostatic potential to a very good agreement with the numerical solution of the Poisson–Boltzmann equation, was worked out for a spherical polyelectrolyte.[36] The correction, W, to the electrostatic potential of eq 17 obeys the following differential equation[36]

$$\nabla^2 W = \kappa^2 (1+f^2)^{1/2} W \quad (19a)$$

$$W(r=0) < \infty \quad (19b)$$

$$W(r \to \infty) = 0 \quad (19c)$$

where κ is the usual Debye–Hückel reciprocal length. For the micelles of the current model, κ is zero in the core and f is zero outside the shell. The continuity of Ψ and its derivative at b and R gives the following expression for the electrostatic potential

$$\frac{e\Psi}{kT} = \frac{e\Psi_o}{kT}\left[1 - (1 + \kappa R)\frac{\sinh[\lambda(r-b)] + \lambda b \cosh[\lambda(r-b)]}{rA} \right] \quad (20a)$$

$$b \le r \le R$$

$$\frac{e\Psi}{kT} = \frac{e\Psi_o}{kT}\frac{Re^{\kappa(R-r)}}{r}\left[1 - (1 + \kappa R)\frac{\sinh(\lambda D) + \lambda b \cosh(\lambda D)}{RA} \right] \quad (20b)$$

$$r \ge R$$

where $\lambda = \kappa(1+f^2)^{1/4}$ and

$$A = (\kappa + \lambda^2 b)\sinh(\lambda D) + \lambda(1+\kappa b)\cosh(\lambda D) \quad (21)$$

The corrected free energy is then

$$\frac{F_{el}}{kT} = \frac{F_{el,o}}{kT} + \frac{3mN\beta}{f}\frac{1+\kappa R}{1-(R/b)^3}\int_0^f \frac{e\Psi_o/kT}{A\lambda b^2}\left[\left(\lambda R - \frac{1}{\lambda R}\right)\sinh(\lambda D) + \frac{D}{b}\cosh(\lambda D) \right] df \quad (22)$$

Finally the interaction free energy is the sum of the electrostatic and van der Waals contributions:

$$F_{int} = F_{el} + F_{vw} \quad (23)$$

3. Micellar Phase

3.1. Translational Free Energy. When polymer molecules associate to form micelles, they lose translational energy. This loss does not favor the formation of micelles with a large number of molecules. To be able to calculate the fraction of micelles of different sizes, one needs to consider the free energy of mixing. The ideal solution mixing free energy for polymers, according to the Flory–Huggins theory, is

$$F_{trans} = \Omega kT\left\{(1-\phi)\ln(1-\phi) + \sum_m \frac{\phi_m}{mN}\ln(\phi_m/mN)\right\} \quad (24)$$

when Ω is the total number of sites, ϕ_m is the volume fraction of micelles of size m, and ϕ is the volume fraction of polymer. The micelle volume fractions, ϕ_m, $m = 1, 2, \ldots$, are related to the polymer volume fraction, ϕ, by

$$\phi = \sum_m \phi_m \quad (25)$$

No enthalpic term is included in eq 24 because the interactions between micelles are assumed negligible at low concentrations.

Table I
Model Parameters

no. of backbone segments, $N = 34$
no. of carbon atoms in the hydrophobic side chains, $N_s = 10$
no. of ethylene oxide groups in the hydrophilic side chains, $N_p = 9$
segment length, $a = 0.5$ nm
interfacial tension, $\gamma = 45$ mN/m
Flory interaction parameter, $\chi = 0.45$
fraction of ionization, $\beta = 0.3$
free energy of side-chain transfer, $\mu = -kT(2.55 + 1.25N_s)$[38]
hydrophobic side-chain volume, in nm^3, $v_s = 0.0274 + 0.0269N_s$[38]
hydrophobic side-chain length, in nm, $l = 0.15 + 0.1265N_s$[38]
volume of hydrophilic side chain, in nm^3, $v_p = 0.032N_p$[39]
length of hydrophilic side chain, in nm, $L = 0.19N_p$[39]
volume of backbone segment, $v_B = 0.0269 \times 4 = 0.1076$ nm^3

3.2. Total Free Energy. The total free energy of the solution is the sum of the contributions from eq 1 and 24

$$F_{total} = \sum_m n_m F_m + F_{trans} \quad (26)$$

where n_m is the number of micelles of size m. At equilibrium, the system free energy is obtained by minimizing eq 26 with respect to all independent variables: n_m, the number of micelles of size m, and D, the thickness of the shell in each micelle size, or, equivalently, the core diameter, b. Since F_{trans} is not dependent on b, minimization of F_{total} with respect to this variable results in finding the optimum b, by minimizing F_m for every size independent of the others (the micelles are assumed to be noninteracting). The one-dimensional minimization is carried out using the golden section method, with the starting values of b/l in the range of 0–1. Minimization of F_{total} with respect to n_m results in the following relation:[37]

$$\phi_m = mN(\phi_1/N)^m \exp[-F_m/kT + mF_1/kT + m - 1] \quad (27)$$

In this equation the energetic term $\exp\{(mF_1 - F_m)/kT\}$ favors the formation of large micelles (large m) when $F_m < mF_1$, while the entropic term $\phi_1{}^m$ favors the formation of small micelles as expected. A maximum in the distribution of micelle size appears where these two opposing forces balance out.

3.3. Properties of the Micellar Phase. The free energies derived in the previous sections form the basis for calculating the properties of the micellar phase, once the polymer parameters and the state variables are known. The model parameters listed in Table I are chosen to mimic the polymer of Figure 1. The hydrophobic side-chain length, l, volume, v_s, and free energy of transfer, μ, are taken from surfactant studies.[38]

Minimization of the total free energy with respect to core radius, which is equivalent to minimization with respect to shell thickness, is performed numerically. The results are reported in Table II as a function of salt concentration. All calculations reported in this work are performed at a temperature of 298 K.

To calculate the volume fraction of each micelle size ϕ_m, one can use eq 25 and 27 and the information in Table II. It is helpful first to examine the formation of micelles with three molecules. According to Table II, ϕ_3 is of the order of 10^{-77} or less (this very small value results from the energetic term in eq 27). As a result, one

Table II
Variation of the Micelle Free Energy F_m, in Units of kT, and Core and Shell Radius R_m with Salt Concentration at $\phi = 0.01$

m	C_s, M	b/l	D/l	$F_m - F_{m,o}$	$mF_1 - F_m$	R_m, nm
1	0.01	0.865	0.422	-200.7	0.0	1.82
1	0.1	0.866	0.417	-214.1	0.0	1.82
1	1.0	0.867	0.412	-220.4	0.0	1.81
2	0.01	1.00	0.703	-409.2	7.8	2.41
2	0.1	1.00	0.703	-438.1	9.9	2.41
2	1.0	1.00	0.703	-450.6	9.8	2.41
3	0.01	1.00	1.00	-470.6	-131.5	2.83
3	0.1	1.00	1.00	-515.2	-127.1	2.83
3	1.0	1.00	1.00	-534.0	-127.2	2.83

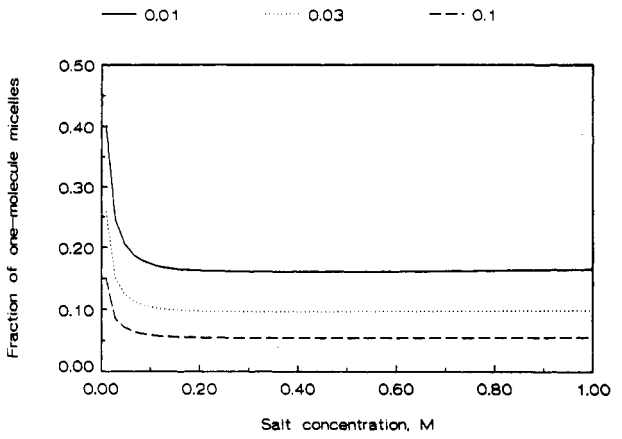

Figure 3. Fraction of one-molecule micelles, ϕ_1/ϕ, as a function of salt concentration for different values of polymer volume fraction. All other parameters are as listed in Table I.

concludes that only one-molecule and two-molecule micelles form for the given conditions. This results in the following expression for the volume fraction of one-molecule micelles

$$\phi_1 = [-1 + (1 + 4\phi E)^{1/2}]/2E \tag{28}$$

where $E = (2/N)\exp[2F_1/kT - F_2/kT + 1]$. For the more general case, which is obtained by combining eq 25 and 27, ϕ_1 is solved numerically. The fraction of one-molecule micelles, ϕ_1/ϕ, is shown in Figure 3 for three values of ϕ. The average core and shell radius is calculated as follows:

$$\bar{R} = \sum_m \phi_m R_m/\phi \tag{29}$$

Note that this is not equal to the micelle radius, which would be R plus the length of the hydrophilic side chain, L. The values of $\bar{R}$ are plotted in Figure 4. The effect of various factors on the micellar phase properties are discussed in more detail in the Discussion.

4. Discussion

In this section the effects of salt and polymer concentrations and some polymer characteristics on the micellar phase composition and mean size are discussed. Consider first the effect of salt concentration. Figure 3 shows the variation of ϕ_1/ϕ with salt concentration up to 1 M. According to this figure, increasing salt concentration tends to favor the formation of multimolecule micelles. This tendency is due to a decrease in the repulsion between backbone segments in the shell region. Figure 4 illustrates the variation of the mean radius, $\bar{R}$, with salt concentration. The average radius increases slightly with increasing salt concentration, a direct result of the formation of more multimolecule micelles that have larger size.

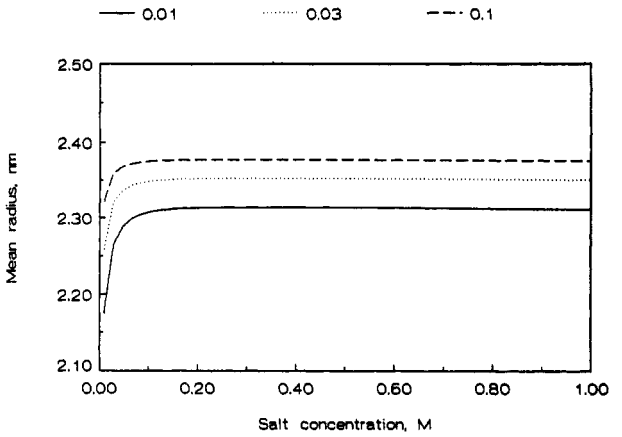

Figure 4. Mean radius, $\bar{R}$, as a function of salt concentration for different values of polymer volume fraction. All other parameters are as listed in Table I.

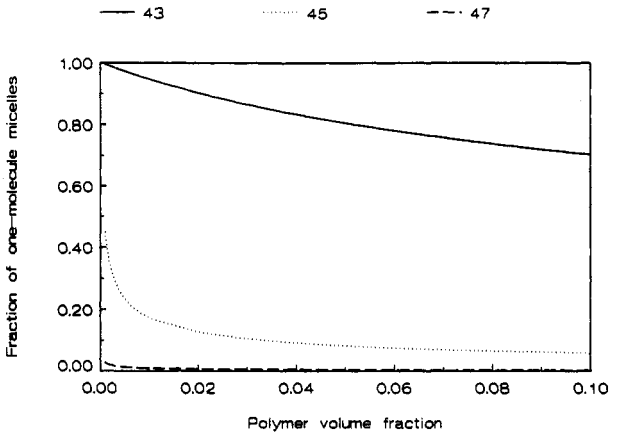

Figure 5. Fraction of one-molecule micelles, ϕ_1/ϕ, as a function of polymer volume fraction. The salt concentration is 0.1 M, and the three curves correspond to interfacial tension, γ, of 43, 45, and 47 mN/m. All other parameters are as listed in Table I.

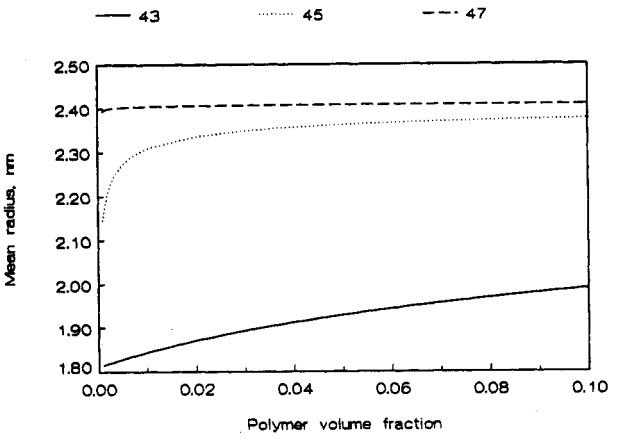

Figure 6. Mean radius, $\bar{R}$, as a function of polymer volume fraction. The salt concentration is 0.1 M, and the three curves correspond to interfacial tension, γ, of 43, 45, and 47 mN/m. All other parameters are as listed in Table I.

Increasing polymer concentration has the same qualitative effect as increasing the salt concentration. This behavior (Figures 5 and 6) results from the decrease in the loss of translational free energy per molecule as the polymer concentration increases. Figures 5 and 6 also show the sensitivity of the micellar phase properties to the value of interfacial tension used in eq 7. The large changes in composition and size with variations in the interfacial tension are due to the exponential dependence of ϕ_m on the free energy difference in eq 27 and the cancellation

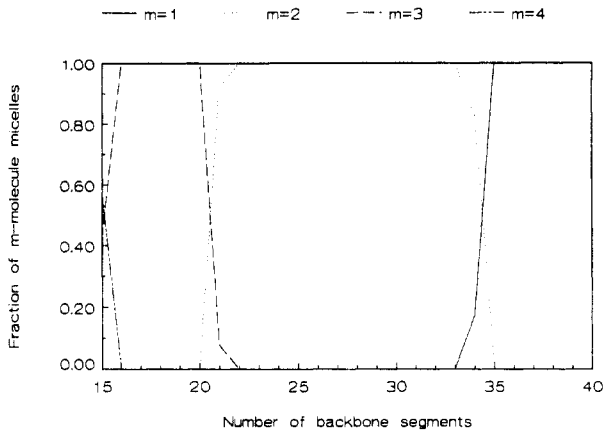

Figure 7. Fractions of m-molecule micelles, ϕ_m/ϕ, as a function of the number of polymer segments. The salt concentration is 0.1 M, and the polymer volume fraction is 0.01. All other parameters are as listed in Table I.

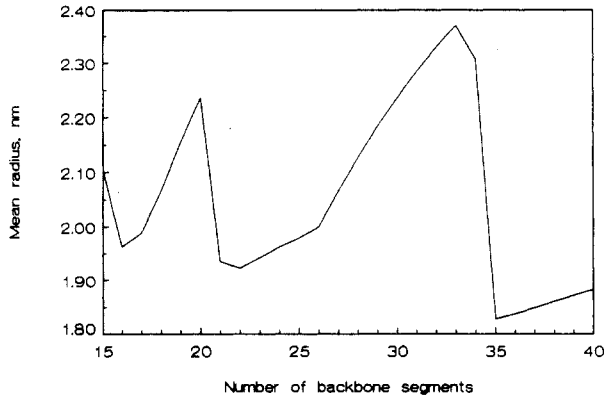

Figure 8. Mean radius, $\bar{R}$, as a function of the number of polymer segments. The salt concentration is 0.1 M, and the polymer volume fraction is 0.01. All other parameters are as listed in Table I.

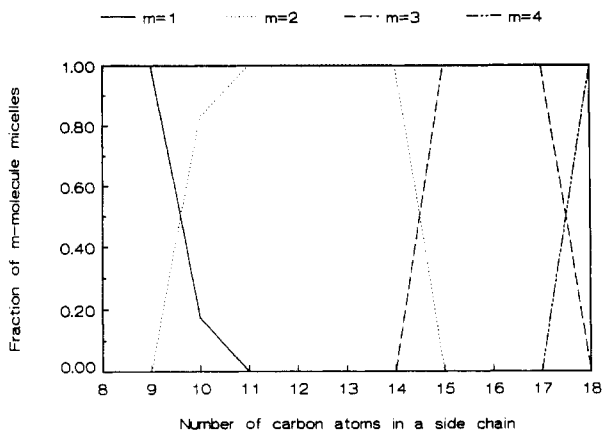

Figure 9. Fractions of m-molecule micelles, ϕ_m/ϕ, as a function of the number of carbon atoms in the hydrophobic side chain. The salt concentration is 0.1 M, and the polymer volume fraction is 0.01. All other parameters are as listed in Table I.

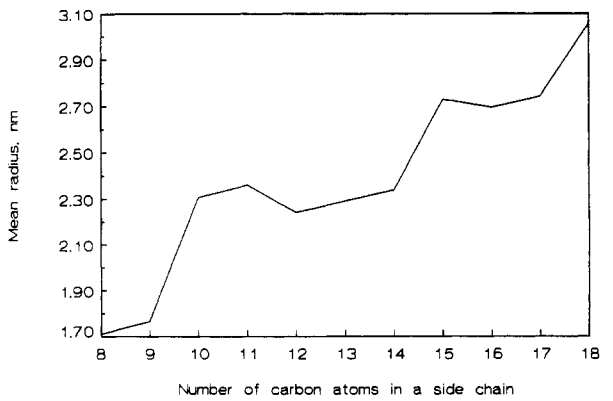

Figure 10. Mean radius, $\bar{R}$, as a function of the number of carbon atoms in the hydrophobic side chain. The salt concentration is 0.1 M, and the polymer volume fraction is 0.01. All other parameters are as listed in Table I.

of the large values of F_m. For example, although the values of $(F_m - F_{m,0})/kT$ are on the order of 10^2, the difference $(2F_1 - F_2)/kT$, which appears in eq 27, is only equal to 7.8 for a salt concentration of 0.01 M (Table II). As a result, small changes in the free energy due to variations in interfacial tension or Flory interaction parameter, for example, will cause sizable changes in micellar properties.

Increasing the number of segments favors the formation of micelles with a smaller number of molecules (Figure 7). In fact beyond $N = 35$ only single molecule micelles form. This follows from the fact that a small number of large polymer molecules (with a large number of hydrophobic side chains) can provide enough protection of the hydrophobic side chains from water. As the size of the molecule gets smaller, more molecules are needed to achieve the same level of protection of the hydrophobic side chains. In addition, as the size of the molecule increases, the shell region becomes overcrowded; this behavior favors the formation of micelles with less molecules. As the number of segments increases, the mean size initially increases with the number of segments, then goes down sharply, and then increases again, and this cycle is repeated twice for N in the range of 16–40 (Figure 8). The initial increase in the size is understandable because of the increase in the molecular size. The sharp decrease in size corresponds to the sharp decrease in the number of three-molecule micelles. The switch from three-molecule micelles to two-molecule micelles causes the sharp decrease in average size, since two-molecule micelles are obviously smaller. This behavior is repeated again when two-molecule micelles disappear and one-molecule micelles dominate.

The effect of the hydrophobic chain length on the fraction of m-molecule micelles is shown in Figure 9. Virtually no multimolecule micelles exist below $N_s = 9$. The ability of more molecules to form a single micelle for longer side chains is a result of two factors. First, the longer side chains form larger cores and hence larger shell volume, which now can accommodate more segments. Second, the backbone segments feel a stronger attractive force because of the longer side chain attached to them. As expected, micelles are larger when the side chains are longer (Figure 10). The sharp increases in size when N_s goes from 10 to 11, 14 to 15, and 17 to 18 are due to the sharp changes in the fraction of micelles containing one-, two-, and three-polymer molecules. The slight decrease in size when N_s goes from 11 to 12 or from 15 to 16 is due to an increase in attraction felt by the backbone segments in two- and three-molecule micelles.

Conclusions and Summary

The microscopic model developed in this work for the formation of micelles by amphiphilic side-chain polymers accounts for the major free-energy contributions in a simple way. The model mimics surfactant micelles in some way because the polymer is essentially a set of connected surfactant molecules. The major difference between surfactant micelles and polymer micelles is the connectivity of the hydrophobic and hydrophilic groups to the polymer backbone. The connectivity does not allow all the

hydrophobic side chains to be fully in the core, contrary to what is observed in surfactant micelles. No critical micellar concentration is observed for moderate values of the number of hydrophobic side chains in a polymer molecule. Significant contributions to the free energy arise from the shell region, which has no equivalence in surfactant micelles. The abrupt changes in micellar size are also due to the connectivity of the hydrophobic groups. In the present model, a number of assumptions were made, some of which are being relaxed in more refined studies in progress. For instance, the hydration of the ethylene oxide moieties needs to be incorporated.

The test for this and any subsequent model would be provided by comparison to experimental results. Data on systems that fall within the applicability of this model will be presented in a separate paper.[28] The current model is not applicable to very long polymers where parts of the backbone have to go into the core with the hydrophobic side chains and polymers with the number of side chains much smaller than the number of segments.

Acknowledgment. This research was supported by a Presidential Young Investigator Award from the National Science Foundation (CBT 85-52882).

References and Notes

(1) Cabane, B.; Duplessix, R. *J. Phys.* (*Les Ulis, Fr.*) **1982**, *43*, 1529; **1987**, *48*, 651.
(2) Goddard, E. D. *Colloids Surf.* **1986**, *19*, 255.
(3) Nagarajan, R.; Kalpakci, B. *Microdomains in Polymer Solutions*; Dubin, P., Ed.; Plenum Press: New York, 1985; p 369.
(4) Qutubuddin, S.; Miller, C. A.; Benton, W. J.; Fort, T. *Macro- and Microemulsions: Theory and Applications*; ACS Symposium Series 272; Shah, D. O., Ed.; American Chemical Society: Washington, DC; 1985; p 223.
(5) Siano, D. B.; Bock, J. *J. Colloid Interface Sci.* **1982**, *90*, 359.
(6) Strauss, U. P.; Gershfeld, N. L. *J. Phys. Chem.* **1956**, *60*, 577.
(7) Inoue, H. *Kolloid Z. Z. Polym.* **1964**, *195*, 102; **1964**, *196*, 1.
(8) Medalia, A. I.; Freedman, H. H.; Sinha, S, K. *J. Polym. Sci.* **1959**, *40*, 15.
(9) Bekturov, E. A.; Bakauova, Z. Kh. *Synthetic Water-Soluble Polymers in Solution*; Huthig & Wepf: Basel, Switzerland, 1986.
(10) Finkelmann, H.; Luhmann, B.; Rehage, G. *Colloid Polym. Sci.* **1982**, *260*, 56.
(11) Luhmann, B.; Finkelmann, H.; Rehage, G. *Angew. Makromol. Chem.* **1984**, *123*, 217.
(12) Sonnessa, A. J.; Cullen, W.; Ander, P. *Macromolecules* **1980**, *13*, 195.
(13) Knapick, E. G.; Hirsch, J. A.; Ander, P. *Macromolecules* **1985**, *18*, 1015.
(14) Shih, L. B.; Sheu, E. Y.; Chen, S. H. *Macromolecules* **1988**, *21*, 1387.
(15) Schulz, D. N.; Kaladas, J. J.; Maurer, J.; Bock, J.; Pace, S. J.; Schulz, W. W. *Polymer* **1987**, *28*, 2110.
(16) Valint, P. L., Jr.; Bock, J. *Macromolecules* **1988**, *21*, 175.
(17) Price, C. *Pure Appl. Chem.* **1983**, *55*, 1563.
(18) Nakagawa, T.; Inoue, H. *Kolloid Z. Z. Polym.* **1964**, *195*, 93.
(19) Kolinski, A.; Skolnick, J.; Yaris, R. *J. Chem. Phys.* **1986**, *85*, 3585.
(20) Stadler, R. *Macromolecules* **1988**, *21*, 121.
(21) Post, C. B.; Zimm, B. H. *Biopolymers* **1979**, *18*, 1487.
(22) Balazs, A. C.; Anderson, C.; Muthukumar, M. *Macromolecules* **1987**, *20*, 1999.
(23) Cates, M. E.; Witten, T. A. *Macromolecules* **1986**, *19*, 732.
(24) Leibler, L.; Orland, H.; Wheeler, J. C. *J. Chem. Phys.* **1983**, *79*, 3550.
(25) ten Brinke, G.; Hadziioannou, G. *Macromolecules* **1987**, *20*, 486.
(26) Munch, M. R.; Gast, A. P. *Macromolecules* **1988**, *21*, 1360.
(27) Halperin, A. *Macromolecules* **1987**, *20*, 2943.
(28) Hamad, E. Z.; Qutubuddin, S., manuscript in preparation.
(29) Hamad, E. Z.; Qutubuddin, S., manuscript in preparation.
(30) de Gennes, P. G. *Scaling Concepts in Polymer Physics*; Cornell University Press: Ithaca, NY, 1979.
(31) Ozisik, M. N. *Heat Conduction*; John Wiley & Sons: New York, 1980; p 168.
(32) Tanford, C. *J. Phys. Chem.* **1959**, *52*, 788.
(33) Kimball, G. E.; Cutler, M.; Samelson, H. *J. Phys. Chem.* **1952**, *56*, 57.
(34) Wall, F. T.; Berkowitz, J. *J. Chem. Phys.* **1957**, *26*, 114.
(35) Lifson, S. *J. Polym. Sci.* **1957**, *23*, 431.
(36) Lifson, S. *J. Chem. Phys.* **1957**, *27*, 700.
(37) Goldstein, R. E. *J. Chem. Phys.* **1986**, *84*, 3367.
(38) Tanford, C. *The Hydrophobic Effect*; John Wiley & Sons: New York, 1980.
(39) Zana, R.; Lang, J. In *Solution Behavior of Surfactants*; Mittal, K. L., Fendler, E. J., Eds.; Plenum Press: New York, 1982; Vol. 2, p 1195.

Registry No. Dapral GE 202 Na, 124153-24-8.